

Photochemical & Photobiological Sciences

Accepted Manuscript



This is an *Accepted Manuscript*, which has been through the Royal Society of Chemistry peer review process and has been accepted for publication.

Accepted Manuscripts are published online shortly after acceptance, before technical editing, formatting and proof reading. Using this free service, authors can make their results available to the community, in citable form, before we publish the edited article. We will replace this *Accepted Manuscript* with the edited and formatted *Advance Article* as soon as it is available.

You can find more information about *Accepted Manuscripts* in the [Information for Authors](#).

Please note that technical editing may introduce minor changes to the text and/or graphics, which may alter content. The journal's standard [Terms & Conditions](#) and the [Ethical guidelines](#) still apply. In no event shall the Royal Society of Chemistry be held responsible for any errors or omissions in this *Accepted Manuscript* or any consequences arising from the use of any information it contains.

Substituent effects on fluorescence properties of thiazolo[4,5-*b*]pyrazine derivatives

Tatsuki Nakagawa,^a Minoru Yamaji,^b Shojiro Maki,^a Haruki Niwa,^a and Takashi Hirano*^a

^a *Department of Engineering Science, Graduate School of Informatics and Engineering, The University of Electro-Communications, Chofu, Tokyo 182-8585, Japan*

^b *Division of Molecular Science, Graduate School of Science and Technology, Gunma University, Kiryu, Gunma 376-8515, Japan*

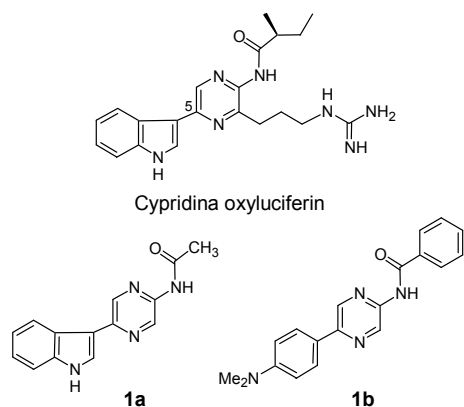
E-mail: thirano@uec.ac.jp; Tel: +81-42-443-5489

Abstract

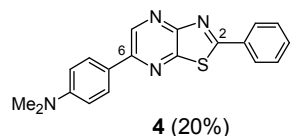
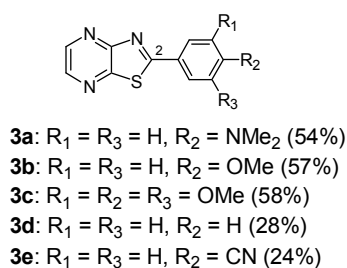
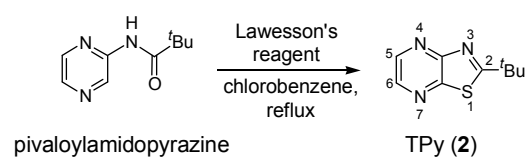
Based on spectroscopic measurements and DFT calculations, fluorescence properties of thiazolo[4,5-*b*]pyrazine (TPy) derivatives having the phenyl group at the C2 position were studied. TPys were readily prepared from the corresponding amidopyrazines, which have a similar fluorescent core to a bioluminescence light emitter, Cypridina oxyluciferin. It was found that introduction of electron-donating (methoxy and dimethylamino) groups onto the 2-phenyl moiety of the TPy derivatives as well as the phenyl and 4-(dimethylamino)phenyl groups at C2 and C6, respectively, is operative for increasing the fluorescence yield and appearance of solvatochromic character. The mechanism of increasing the fluorescence yield depending on the substituents is discussed. These findings provide useful information on designing new TPy fluorophores.

Introduction

Bioluminescent molecular systems show light emission with performance of color variation, high efficiencies, and reactivity controlled for making a desired luminescence pattern.¹ The bioluminescence-related compounds are, therefore, attractive prototypes for designing photon-producing compounds. Cypridina oxyluciferin (Scheme 1), which is the key compound emitting bioluminescence in the ostracod *Cypridina*,² is one of the prototypes for fluorophores.³ It has the amidopyrazine structure as the fluorescent core together with three appendages including the electron-donating 3-indolyl group at C5. One of our goals is to design a new fluorophore using Cypridina oxyluciferin for assisting developments in fluorophore applications such as biological imaging with fluorescent sensors and light-emitting device technology with light-emitting components.⁴ We, therefore, have been investigating the fluorescent properties of Cypridina oxyluciferin analogues **1a** and **1b** (Scheme 1),^{3,5} and also developed a novel fluorophore prepared by chemical modification of the amidopyrazine structure such as difluoro[amidopyrazinato-*O,N*]boron derivatives prepared by a similar method for the synthesis of boron dipyrromethene (BODIPY).⁶ Thiazolo[4,5-*b*]pyrazine (TPy) derivatives are readily prepared from amidopyrazines by the method with Lawesson's reagent reported by Fruit et al. (Scheme 2).⁷ While TPys have been subjected mainly to their pharmaceutical applications,^{7,8} we have paid much attention to their potentials as fluorophores. As benzo-fused TPy derivatives have fluorescence character,⁹ we expect that TPy derivatives may be the key compounds for designing useful fluorophores. In the present work, we introduced the phenyl group at C2 of the TPy ring, which is subjected to investigate substituent effects on the spectroscopic properties for searching for fluorescence appearance (Scheme 2). In addition to the 2-phenyl derivatives **3**, the derivative **4** derived from the Cypridina oxyluciferin analogue **1b** were also investigated. We report herein relationship between the molecular structure and the fluorescent properties of the substituted TPy derivatives for obtaining information on designing new fluorophores having the TPy structure.



Scheme 1. Cypridina oxyluciferin and its analogues **1a** and **b**.



Scheme 2. Synthesis and molecular structures of the TPy derivatives **2**, **3a-e** and **4**.

Experimental

General

Melting points were determined with a Yamato MP-21 apparatus. IR spectra were measured with a Horiba FT-720 spectrometer. High-resolution electro-spray ionization (ESI) mass spectra were recorded on a JEOL JMS-T100LC mass spectrometer. 1H NMR spectra were recorded on a JEOL ECA-500 instrument (500 MHz). UV/visible absorption spectra were measured with a Varian Cary 50 spectrophotometer (scan speed, 600 nm/min; data interval, 1 nm). Fluorescence spectra and fluorescence quantum yields were obtained with a Hamamatsu

Photonics Quantaaurus-QY absolute PL quantum yields measurement system. Fluorescence lifetimes (τ_f) were measured with a Hamamatsu Photonics TAU time-correlated single-photon counting fluorimeter system. Phosphorescence spectra at 77 K were recorded on a Hitachi Fluorescence Spectrometer F-7000 equipped with a 40 Hz mechanical chopper. Spectroscopic measurements were performed in a quartz cuvette (1 cm path length) at 25 ± 1 °C. Spectral-grade solvents were used for the measurements of UV/visible absorption and fluorescence. Third harmonics (355 nm) from a Nd:YAG laser system (20 mJ / pulse, Lotis-TII, LT-2137) and a 400 nm laser pulse (10 mJ / pulse) from a Ti:Sapphire laser system (Lotis-TII, LT-2211) pumped with second harmonics (532 nm) from the Nd:YAG laser system were used as the excitation laser light sources. The details of the detection system for the time profiles of the transient absorption have been reported elsewhere.¹⁰ The temporal data of absorbance changes were analyzed by using the least-squares best-fitting method. Density functional theory (DFT) calculations were performed using the Gaussian 09 program.¹¹ DFT includes Beck's three-parameter function combined with Lee, Yang and Parr's correlation function (B3LYP) along with the 6-31G(d) basis set.¹² Molecular graphics were generated using GaussView, Version 5.¹³

Preparation of the TPy derivatives **3a-e** and **4**

By using the synthesis method for *t*-butyl derivative **2**,⁷ the derivatives **3a-e** having the phenyl group at C2 were prepared by thiocarbonylation and the following thiazole ring formation of the corresponding amidopyrazines with Lawesson's reagent [2,4-bis(4-methoxyphenyl)-1,3-dithia-2,4-diphosphetane 2,4-disulfide] in one pot in 24–58% yields (Scheme 2). Similarly, the TPy derivative **4** was prepared from the Cypridina oxyluciferin analogue **1b**³ in 20% yield.

4-(Dimethylamino)benzamidopyrazine. To a solution of aminopyrazine (200 mg, 2.1 mmol) in pyridine (0.7 mL), 4-(dimethylamino)benzoyl chloride (463mg, 2.5 mol) was added under Ar, and the reaction mixture was heated under reflux for 48 h. The reaction was quenched by adding water (60 mL), and the product was extracted with chloroform (60 mL ×

5). The organic layer was washed with brine, dried over Na₂SO₄, and concentrated in vacuo. The residue was purified by silica gel column chromatography [CHCl₃/methanol (12:1)] and silica gel thin layer chromatography [CHCl₃/ethyl acetate (1:1)], to give 4-(dimethylamino)benzamidopyrazine (176 mg, 35%) as brown crystals: mp 138–139 °C. δ_{H} (CDCl₃) 3.07 (6 H, s), 6.72 (2 H, d, *J* 9 Hz), 7.83 (2 H, d, *J* 9 Hz), 8.24 (1 H, m), 8.32 (1 H, d, *J* 2.9 Hz), 8.34 (1 H, br s) and 9.71 (1 H, d, *J* 1.2 Hz). ν (KBr)/cm⁻¹ 2900, 1668, 1606, 1533, 1413 and 1295. *m/z* (ESI) 243 ([M+H]⁺).

3,4,5-Trimethoxybenzamidopyrazine: 62% yield. Colorless crystals, mp 138–139 °C. δ_{H} (CDCl₃) 3.92 (3 H, s), 3.94 (6 H, s), 7.14 (2 H, s), 8.29 (1 H, m), 8.40 (1 H, d, *J* 2.9 Hz) and 9.70 (1 H, d, *J* 1.2 Hz). ν (KBr)/cm⁻¹ 1674, 1540, 1413, 1338 and 1300. *m/z* (ESI) 195 ([M+H]⁺).

2-(4-Dimethylaminophenyl)thiazolo[4,5-*b*]pyrazine (3a). To a solution of 4-(dimethylamino)benzamidopyrazine (120 mg, 0.50 mmol) in chlorobenzene (1.0 mL), Lawesson's reagent (120 mg, 0.30 mmol) was added and the reaction mixture was heated under reflux overnight. For completing the reaction, Lawesson's reagent (120 mg, 0.30 mmol) was added again, and the solution was heated under reflux for 3 h. The reaction mixture was directly purified by silica gel thin layer chromatography [CHCl₃/ethyl acetate (5:1)], to give **3a** (70 mg, 54%) as yellow crystals: mp 198–199 °C. δ_{H} (CDCl₃) 3.10 (6 H, s), 6.75 (2 H, d, *J* 8.6 Hz), 8.06 (2 H, d, *J* 9.2 Hz), 8.36 (1 H, d, *J* 2.9 Hz) and 8.59 (1 H, d, *J* 2.3 Hz). ν (KBr)/cm⁻¹ 2958, 1600, 1427, 1340 and 1174. *m/z* (ESI) Found: 279.0642 ([M+Na]⁺). C₁₃H₁₂N₄NaS requires 279.0680.

2-(4-Methoxyphenyl)thiazolo[4,5-*b*]pyrazine (3b): 57% yield. Yellow crystals, mp 178–179 °C. δ_{H} (CDCl₃) 3.91 (3 H, s), 7.04 (2 H, d, *J* 8.6 Hz), 8.16 (2 H, d, *J* 8.6 Hz), 8.45 (1 H, d, *J* 2.9 Hz) and 8.64 (1 H, d, *J* 2.3 Hz). ν (KBr)/cm⁻¹ 1606, 1511, 1457, 1344, 1265 and 1174. *m/z* (ESI) Found: 266.0347 ([M+Na]⁺). C₁₂H₉N₃NaOS requires 266.0364.

2-(3,4,5-Trimethoxyphenyl)thiazolo[4,5-*b*]pyrazine (3c): 58% yield. Yellow crystals, mp 175–176 °C. δ_{H} (CDCl₃) 3.95 (3 H, s), 3.99 (6 H, s), 7.45 (2 H, s), 8.50 (1 H, d, *J* 2.9 Hz)

and 8.68 (1 H, d, J 2.9 Hz). ν (KBr)/ cm^{-1} 2958, 1587, 1463, 1342, 1248, 1191 and 1122. m/z (ESI) Found: 326.0544 ($[\text{M}+\text{Na}]^+$). $\text{C}_{14}\text{H}_{13}\text{N}_3\text{NaO}_3\text{S}$ requires 326.0575.

2-Phenylthiazolo[4,5-*b*]pyrazine (3d): 28% yield. Yellow crystals, mp 122–123 °C. δ_{H} (CDCl_3) 7.55 (2 H, m), 7.59 (1 H, m), 8.21 (2 H, m), 8.51 (1 H, d, J 2.8 Hz) and 8.69 (1 H, d, J 2.3 Hz). ν (KBr)/ cm^{-1} 1533, 1469, 1342, 1232 and 1184. m/z (ESI) Found: 236.0295 ($[\text{M}+\text{Na}]^+$). $\text{C}_{11}\text{H}_7\text{N}_3\text{NaS}$ requires 236.0258.

2-(4-Cyanophenyl)thiazolo[4,5-*b*]pyrazine (3e): 24% yield. Yellow crystals, mp 237–238 °C. δ_{H} (CDCl_3) 7.85 (2 H, d, J 8.6 Hz), 8.32 (2 H, d, J 8.6 Hz), 8.59 (1 H, d, J 2.9 Hz) and 8.76 (1 H, d, J 2.8 Hz). ν (KBr)/ cm^{-1} 2231, 1533, 1455, 1340 and 1190. m/z (ESI) Found: 239.0379 ($[\text{M}+\text{H}]^+$). $\text{C}_{12}\text{H}_7\text{N}_4\text{S}$ requires 239.0391.

6-(4-Dimethylaminophenyl)-2-phenylthiazolo[4,5-*b*]pyrazine (4): 20% yield. Orange crystals, mp 231–233 °C. δ_{H} (CDCl_3) 3.07 (6 H, s), 6.82 (2 H, d, J 8.6 Hz), 7.52–7.56 (3 H, m), 8.03 (2 H, d, J 8.6 Hz), 8.19 (2 H, m) and 9.05 (1 H, s). ν (KBr)/ cm^{-1} 1604, 1535, 1465, 1328 and 1193. m/z (ESI) Found: 355.0961 ($[\text{M}+\text{Na}]^+$). $\text{C}_{19}\text{H}_{16}\text{N}_4\text{NaS}$ requires 355.0993.

Results and discussion

Spectroscopic properties of TPy derivatives

Figure 1 shows absorption and fluorescence spectra of **3a-c** and **4** in various solvents. The data of UV/visible absorption and fluorescence are summarized along with the used $E_{\text{T}}(30)$ index¹⁴ in Tables 1 and 2, respectively. Fluorescence was not seen from the *t*-butyl derivative **2**, phenyl derivative **3d** and 4-cyanophenyl derivative **3e** while the derivatives **3a-c** having the electron-donating group(s) on the 2-phenyl ring showed fluorescence with appreciable quantum yields ($\Phi_{\text{f}} \geq 0.005$) in the used solvents. Although the 2-phenyl derivative **3d** is nonfluorescent, the 2-phenyl derivative **4** having the additional 6-phenyl ring substituted with the electron-donating group fluoresces with relatively large quantum yields ($\Phi_{\text{f}} \geq 0.1$). The absence and presence of fluorescence in cyclohexane solution indicate that the electronic character in the lowest excited singlet (S_1) states of **3a-c** and **4** is of π, π^* whereas that of **2**, **3d** and **3e** is of n, π^* . The fluorescence maximum wavelengths (λ_{fl}) and Φ_{f} of **3a-c** and **4** vary depending on the solvent polarity. From the 0-0 origins of absorption and fluorescence spectra

in cyclohexane, the S_1 state energies (E_S) of **3a**, **3b**, **3c** and **4** were, respectively, determined to be 71.2, 78.4, 76.8 and 65.2 kcal mol⁻¹ (Table 3). As an increase of the $E_T(30)$, the λ_{fl} undergoes a red shift while we can recognize a decrease of the Φ_f in **3a** and **4** having the 4-(dimethylamino)phenyl group and an increase of the Φ_f in **3b** and **3c** having the methoxy-substituted phenyl group. These results indicate that the introduction of the electron donating phenyl group to the TPy ring is clue for inducing fluorescence character, probably, due to charge-transfer (CT) interaction in the π -electronic molecular structure which causes bathochromic shifts and changes in the λ_{fl} values.

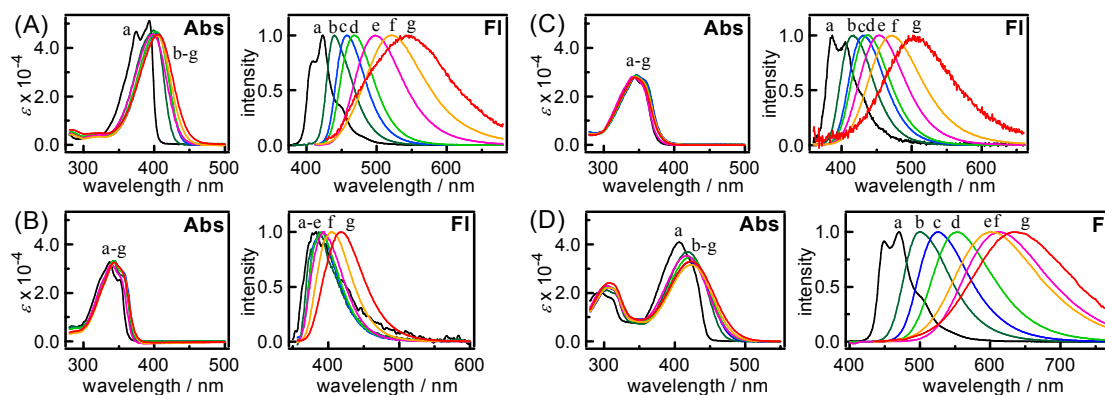


Figure 1. UV/visible absorption (Abs) and fluorescence (Fl) spectra of **3a** (A), **3b** (B), **3c** (C) and **4** (D) in cyclohexane (a), benzene (b), chloroform (c), dichloromethane (d), acetonitrile (e), 2-propanol (f) and methanol (g) at 298 K.

Table 1. Electronic absorption properties of **2–4** in various solvents at 298 K.

solvent [$E_T(30)^a$]	$\lambda_{ab} / \text{nm} (\epsilon / 10^4 \text{ dm}^3 \text{ mol}^{-1} \text{ cm}^{-1})^b$						
	2	3a	3b	3c	3d	3e	4
cyclohexane	296 (1.10)	393 (5.13)	351 (2.54)	342 (2.81)	322 (2.57)	322 (2.78)	407 (4.09)
[30.9]		375 (4.68)	337 (3.28)				295 (2.03)
benzene	297 (1.07)	399 (4.72)	342 (3.32)	347 (2.89)	325 (2.50)	331 (2.71)	418 (3.70)
[34.3]							304 (2.11)
chloroform	---	404 (4.62)	344 (3.32)	347 (2.86)	---	---	422 (3.28)
[39.1]							306 (2.20)
dichloromethane	---	403 (4.67)	342 (3.33)	345 (2.85)	---	---	420 (3.47)
[40.7]							305 (2.28)
acetonitrile	296 (1.11)	398 (4.57)	339 (3.17)	342 (2.82)	322 (2.50)	328 (2.90)	417 (3.53)
[45.6]							303 (2.29)
2-propanol	---	404 (4.51)	344 (3.25)	345 (2.81)	---	---	424 (3.16)
[48.4]							306 (2.21)
methanol	---	406 (4.56)	343 (3.26)	344 (2.78)	---	---	424 (3.30)
[55.4]							307 (2.41)

a) $E_T(30)$ in kcal mol⁻¹. b) Absorption maximum (λ_{ab}) and extinction coefficient (ϵ) in dm³ mol⁻¹ cm⁻¹ in parenthesis.

Table 2. Fluorescence properties of **3a-c** and **4** in various solvents at 298 K.

solvent [$E_T(30)$]	λ_{fl} / nm (Φ_f) ^a			
	3a	3b	3c	4
cyclohexane [30.9]	410, 423 (0.46)	~380 (0.005)	386, 405 (0.023)	449, 470 (0.89)
benzene [34.3]	440 (0.91)	386 (0.011)	417 (0.23)	499 (0.78)
chloroform [39.1]	457 (0.91)	392 (0.032)	430 (0.63)	526 (0.81)
dichloromethane [40.7]	468 (0.94)	390 (0.031)	436 (0.65)	553 (0.78)
acetonitrile [45.6]	498 (0.86)	392 (0.034)	455 (0.74)	610 (0.28)
2-propanol [48.4]	520 (0.25)	404 (0.11)	472 (0.54)	601 (0.11)
methanol [55.4]	542 (0.012)	418 (0.31)	501 (0.042)	634 (0.008)

a) Fluorescence maximum wavelengths (λ_{fl}) and quantum yields (Φ_f) in parenthesis.

In contrast to the λ_{fl} values of **3a-c** and **4**, the absorption maxima (λ_{ab}) of the lowest energy absorption bands were not apparently dependent on the solvent variation. The fluorescence solvatochromism may be caused by the polarized character in the excited singlet (S_1) states of **3a-c** and **4** compared to that in the corresponding ground (S_0) states. The variation in the fluorescence spectra of **3a-c** and **4** was evaluated by correlating the fluorescent state energies (E_{fl} in kcal mol⁻¹) with $E_T(30)$ (Figure 2). The plots of E_{fl} as a function of $E_T(30)$ show linear correlations with correlation coefficients (r) of the lines; $E_{fl} = -0.63E_T(30) + 87$ ($r = -0.99$) for **3a**, $E_{fl} = -0.26E_T(30) + 83$ ($r = -0.95$) for **3b**, $E_{fl} = -0.56E_T(30) + 88$ ($r = -1.00$) for **3c** and $E_{fl} = -0.67E_T(30) + 80$ ($r = -0.96$) for **4**. The negative slopes of the plots are evident for the enhanced dipolar character of the S_1 states of **3a-c** and **4**. The slopes of the linear correlations for **3a** and **4** are greater than those for **3b** and **3c**, indicating that the strength in dipolar character of the S_1 states is enhanced by introduction of the dimethylamino group compared to that of the methoxy group(s). Thus, introducing the 4-(dimethylamino)phenyl group to the TPy ring at the C2 and C6 positions is effective for appearance of the fluorescence solvatochromism. **3a** and **4** show wide variation ranges (410–542 and 449–634 nm, respectively) in the λ_{fl} values depending on the solvent polarity. The Φ_f values of **3a** and **4** in aprotic solvents are substantially greater than those in protic solvents. The highly polarized S_1 states of **3a** and **4** in aprotic solvents seem to be deactivated by hydrogen

bonding interactions.

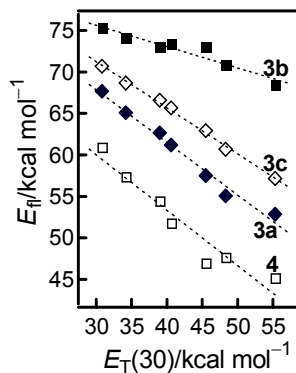


Figure 2. E_{f1} values of **3a** (◆), **3b** (■), **3c** (◇) and **4** (□) plotted as a function of $E_{T(30)}$.

Fluorescent properties of TPy derivatives

To reveal what governs spectroscopic properties of TPy derivatives, fluorescence lifetimes (τ_f) of **3a-c** and **4** in cyclohexane were measured (Table 3). Based on the τ_f values, the rate constants (k_f) of the fluorescence emission process were estimated using the equation, $k_f = \Phi_f \tau_f^{-1}$. The quantum yields (Φ_{nr}) and rate constants (k_{nr}) of the nonradiative decay processes were estimated according to the equations, $\Phi_{nr} = 1 - \Phi_f$ and $k_{nr} = \Phi_{nr} \tau_f^{-1}$, respectively. As to the derivatives **3a** and **4** having the 4-(dimethylamino)phenyl group, the k_f values are comparative to the k_{nr} values, indicating that the fluorescence process is competitive with the nonradiative ones. In contrast, although we are unable to determine the definite values of k_f and k_{nr} due to the short fluorescence lifetimes of the derivatives **3b** and **3c** with the methoxy-substituted phenyl group with our instruments, it seems that the nonradiative process is dominant in the deactivation process from the S_1 states. Therefore, the reason why the Φ_f values of **3a** and **4** are greater than those of **3b** and **3c** is that the electron donation from the 4-(dimethylamino)phenyl group to the TPy core reduces the rate of the nonradiative process in the S_1 state while the electron donation from the methoxy-substituted phenyl group is less efficient for the reduction.

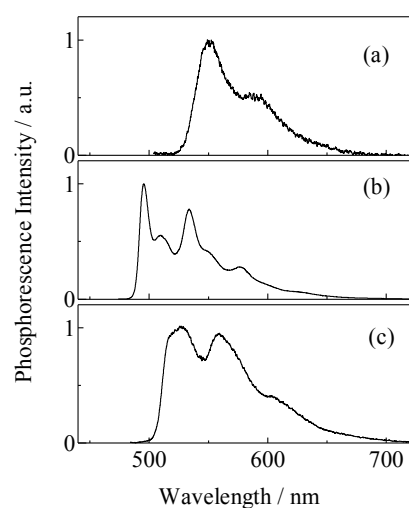
Table 3. Photophysical properties of **3a-c** and **4** in cyclohexane at 295 K.

Compounds	λ_{abs} / nm	λ_{fl} / nm	$\lambda_{\text{ex}}^{\text{a}}$ / nm	E_{S}^{b} / kcal mol ⁻¹	$\Phi_{\text{nr}}^{\text{c}}$	Φ_{f}	τ_{f} / ns	k_{f}^{d} / 10 ⁸ s ⁻¹	k_{nr}^{e} / 10 ⁸ s ⁻¹	E_{T}^{f} / kcal mol ⁻¹
3a	393, 375	410, 423	365	71.2	0.54	0.46	0.97	4.7	5.6	51.9
3b	351, 337	~390	365	78.4	0.99	0.006	<0.3	>0.2	>30	57.6
3c	342	405, 486	340	76.8	0.98	0.023	<0.3	>0.8	>30	55.2
4	407	449, 470	405	65.2	0.11	0.89	2.3	3.9	0.48	-

a) Excitation wavelengths. b) The S₁ state energies determined from the 0-0 origins of absorption and fluorescence spectra. c) Determined by $\Phi_{\text{nr}} = 1 - \Phi_{\text{f}}$. d) Determined by $k_{\text{f}} = \Phi_{\text{f}} \tau_{\text{f}}^{-1}$. e) Determined by $k_{\text{nr}} = \Phi_{\text{nr}} \tau_{\text{f}}^{-1}$. f) The T₁ state energies determined from the phosphorescence spectra in ethanol at 77 K.

Phosphorescence and transient absorption measurements

To understand the nonradiative processes from the S₁ states of **3a-c** and **4**, we investigated the triplet state formation by phosphorescence and transient absorption measurements. Phosphorescence from **3a-c** in ethanol at 77 K was observed as shown in Figure 3 whereas phosphorescence was absent from **4** in the wavelength region, 450–750 nm. The phosphorescence spectrum of **3b** shows steep vibrational structures which are characteristic of n,π*. Conversely, **3a** and **3c** give broad phosphorescence spectra due to π,π* character. From the 0-0 origins of the phosphorescence spectra, the triplet energies (E_T) of **3a**, **3b** and **3c** are, respectively, determined to be 51.9, 57.6 and 55.2 kcal mol⁻¹. Observation of phosphorescence indicates that intersystem crossing from the S₁ to the lowest triplet (T₁) state efficiently proceeds in **3a-c**.

**Figure 3.** Phosphorescence spectra of **3a** (a), **3b** (b) and **3c** (c) in ethanol at 77 K.

Transient absorption spectra were obtained upon laser photolysis of **3a-c** and **4** in deaerated cyclohexane at 295 K (Figures 4a-d). The intensities of the transient signals decreased with lifetimes in the microsecond time domain (**3a**; 760 ns, **3b**; 7.4 μ s, **3c**; 420 ns and **4**; 1.4 μ s). The decay lifetimes were shortened on exposing the solution to the air. In acetonitrile solution of **3b** and **3c**, transient absorption spectra similar to those in cyclohexane were obtained (the spectra are deposited in the Electronic Supplementary Information) although we observed weak transient absorption for **3a** and **4** in acetonitrile (Figures 3e and 3f). The features of the transient absorption spectra in acetonitrile were different from those obtained in cyclohexane whereas they resemble each other. The transient signals for **3a** and **4** in acetonitrile decreased with lifetimes of 1.0 and 1.3 μ s, respectively, and they were quenched by the dissolved oxygen. Based on these observations, the transient absorption spectra obtained in cyclohexane and acetonitrile are ascribable to the corresponding T_1 states (triplet-triplet (T-T) absorption), indicating that nonradiative deactivation of the S_1 state in **3a-c** and **4** is mainly governed by intersystem crossing (ISC) to the triplet state. We can, thus, say that the ISC yields of **3a-c** and **4** are equivalent to the estimated Φ_{nr} values. Actually, the intensities of the T-T absorption of **3b** and **3c** in cyclohexane ($\Phi_{nr} \geq 0.98$) are relatively larger than those of **3a** and **4** ($\Phi_{nr} = 0.1\sim 0.5$). It seems that absorption spectrum shapes of triplet 2-phenylTPys sensitively depend on the difference in the number and the positions of the substituent group. The T-T absorption spectra of **3a** and **4** also depend on the solvent polarity. These findings indicate that CT character appears in the T_1 states of **3a** and **4** in fluid polar media.

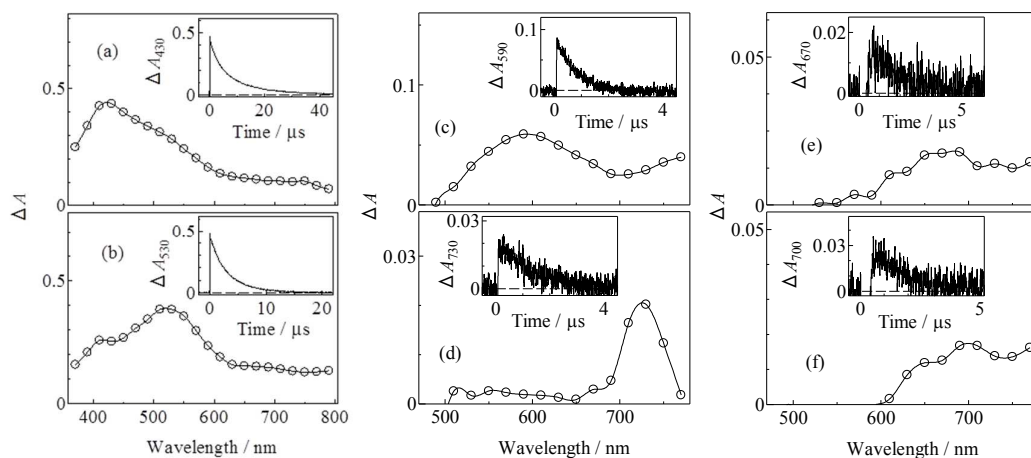


Figure 4. Transient absorption spectra at 500 ns upon 355 nm laser pulsing in cyclohexane solutions of **3b** (a) and **3c** (b), at 300 ns upon 400 nm laser pulsing in cyclohexane solutions of **3a** (c) and **4** (d) and at 900 ns upon 400 nm laser pulsing in Ar-purged acetonitrile solutions of **3a** (e) and **4** (f) obtained at 295 K. Insets; time profiles at 430 nm (a), 530 nm (b), 590 nm (c), 730 nm (d), 670 nm (e) and 700 nm (f).

DFT calculations

DFT and TD-DFT calculations for the electronic characteristics of **2–4** were carried out using the B3LYP/6-31G(d) method. The results summarized in Table 4 show that 1) the $S_0 \rightarrow S_1$ transitions in the non-fluorescent derivatives **2**, **3d** and **3e** together with the weakly fluorescent derivative **3b** are of n,π^* , 2) the $S_0 \rightarrow S_1$ transitions in **3a**, **3c** and **4** are of π,π^* , and 3) the $S_0 \rightarrow S_2$ and $S_0 \rightarrow S_3$ transitions in **3a**, **3c** and **4** are of n,π^* . The oscillator strengths (f) value for the $S_0 \rightarrow S_n$ ($n \geq 1$) transition is related to the extinction coefficient (ε) of the electronic absorption.¹⁵ Obviously, the f values smaller than 0.002 are responsible for the n,π^* forbidden transitions while the ε values of the observed lowest energy absorption bands being in the magnitude of $10^4 \text{ dm}^3 \text{ mol}^{-1} \text{ cm}^{-1}$ are due to the allowed π,π^* transitions. The relative variation in the λ_{ab} and ε values of **2–4** from the absorption measurements is correlated with that in the f values and the wavelengths (λ_{tr}) estimated from the calculated transition energies.

Table 4 Calculation data of **2–4** with DFT and TD-DFT using B3LYP/6-31G(d)

Compound	HOMO /eV	LUMO /eV	n-orbital ^a (ΔE_n^b /eV)	transitions ^c	λ_{tr}^d / nm (f)	configuration ^{a,e}
2	-6.84	-1.75	H (0.00)	$S_0 \rightarrow S_1$ (n,π^*)	323 (0.002)	H \rightarrow L (0.70)
				$S_0 \rightarrow S_3$ (π,π^*)	264 (0.15)	H-1 \rightarrow L (0.61) H-1 \rightarrow L+1 (-0.10) H-2 \rightarrow L (-0.27) H-2 \rightarrow L+1 (-0.16)
3a	-5.36	-1.73	H-1 (1.19)	$S_0 \rightarrow S_1$ (π,π^*)	364 (0.82)	H \rightarrow L (0.70)
				$S_0 \rightarrow S_2$ (n,π^*)	332 (0.001)	H-1 \rightarrow L (0.69) H-1 \rightarrow L+1 (-0.12)
3b	-6.01	-1.97	H-1 (0.74)	$S_0 \rightarrow S_1$ (n,π^*)	335 (0.001)	H-1 \rightarrow L (0.69) H-1 \rightarrow L+1 (-0.12)
				$S_0 \rightarrow S_2$ (π,π^*)	328 (0.77)	H \rightarrow L (0.70)
3c	-5.87	-2.06	H-2 (0.95)	$S_0 \rightarrow S_1$ (π,π^*)	350 (0.53)	H \rightarrow L (0.68) H-1 \rightarrow L (0.14)
				$S_0 \rightarrow S_2$ (n,π^*)	337 (0.001)	H-2 \rightarrow L (0.69) H-2 \rightarrow L+1 (-0.12)

3d	-6.50	-2.17	H-1 (0.38)	$S_0 \rightarrow S_1 (n,\pi^*)$	340 (0.001)	H-1 \rightarrow L (0.69)
						H-1 \rightarrow L+1 (-0.12)
3e	-6.92	-2.78	H-1 (0.29)	$S_0 \rightarrow S_2 (\pi,\pi^*)$	308 (0.63)	H \rightarrow L (0.69)
				$S_0 \rightarrow S_1 (n,\pi^*)$	356 (0.001)	H-1 \rightarrow L (0.69)
4	-5.12	-1.94	H-2 (1.42)	$S_0 \rightarrow S_2 (\pi,\pi^*)$	321 (0.81)	H-1 \rightarrow L+1 (0.14)
				$S_0 \rightarrow S_1 (\pi,\pi^*)$	426 (0.77)	H \rightarrow L (0.69)
				$S_0 \rightarrow S_1 (\pi,\pi^*)$	426 (0.77)	H \rightarrow L (0.70)
				$S_0 \rightarrow S_2 (n,\pi^*)$	346 (0.001)	H-2 \rightarrow L (0.69)
						H-2 \rightarrow L+1 (-0.11)

a) H, H- n ($n = 1$ and 2), L, L+1 denote the HOMO, HOMO- n ($n = 1$ and 2), LUMO, and LUMO+1, respectively. b) Energy difference between HOMO and n-orbital. c) The π,π^* and n,π^* transitions to the excited singlet states with the lowest excitation energies. Character of the transitions is in the parentheses. d) Wavelength estimated from transition energies. e) Configuration of excitation. Coefficients are in the parentheses.

The electronic configuration (π,π^*) of the S_1 states for **3a-c** and **4** concluded by the fluorescence observations are in agreement with the results of the TD-DFT calculations except for **3b**. We have assigned the T_1 states of **3a** and **4** being of π,π^* and triplet **3b** being of n,π^* in nature from the phosphorescence spectral features. According to the El-Sayed's selection rule,¹⁶ the evaluated k_{nr} values, which are equivalent to those of ISC, for **3a-c** and **4** are rationalized. That is, the k_{nr} values of **3b** and **3c** ($> 10^9 \text{ s}^{-1}$) evaluated in cyclohexane at 295 K are for the allowed transition from $^1(\pi,\pi^*)$ to $^3(n,\pi^*)$ whereas those for **3a** and **4** ($< 10^8 \text{ s}^{-1}$) are for the forbidden transition from $^1(\pi,\pi^*)$ to $^3(\pi,\pi^*)$. As for the ISC process from the $S_1(\pi,\pi^*)$ to the $T_1(\pi,\pi^*)$ in **3c**, we suppose that the $T_2(n,\pi^*)$ state close to the T_1 in energy may act as the intermediate, that is, a fast ISC from the $S_1(\pi,\pi^*)$ state to the $T_2(n,\pi^*)$ state, followed by internal conversion to the $T_1(\pi,\pi^*)$.

Assignment and the energy levels of the n-orbitals in the TPy derivatives **2-4** have been revealed by computations (Table 4). We propose that energy differences (ΔE_n) between HOMO and n-orbital (HOMO, HOMO-1 and HOMO-2) may be useful for designing intensively fluorescent TPy derivatives where electronic configuration in the S_1 state being of π,π^* is necessary. The ΔE_n values of the non- and weakly fluorescent **2** and **3b-e** are less than 1.0 eV while those of the fluorescent **3a** and **4** are greater than 1.1 eV. There may be a threshold value being at 1.1 eV in ΔE_n for predicting fluorescent TPys. The term, ΔE_n could be a measure on designing a new TPy fluorophore.

Conclusion

The TPy derivatives **3a** and **4** having the electron-donating 4-(dimethylamino)phenyl group

provide intensive fluorescence with Φ_f values depending on the solvent polarities, and **3b** and **3c** are weakly fluorescent whereas **2**, **3d** and **3e** do not emit. These spectroscopic features indicate that the electronic character in the S_1 states of **3a-c** and **4** is of π,π^* whereas that of **2**, **3d** and **3e** is of n,π^* . The variation in the substituent on the phenyl group at C2 effectively modulates the λ_{fl} and Φ_f values. Increasing the electron-donating property of the substituted phenyl group leads to the bathochromic shift in the λ_{fl} value and an increase of the Φ_f value. In addition, the derivatives **3a-c** show solvatochromism in the fluorescence originated from polarized character of the S_1 states. Consequently, the electron donating from the 4-(dimethylamino)phenyl groups at C2 and C6 of **3a** and **4** to the TPy core is a clue for increasing fluorescent character. Fluorescence efficiencies of **3a-c** and **4** are mainly controlled by the electronic configurations of the triplets via ISC. Transient absorption and phosphorescence measurements for **3a-c** and **4** indicate that their main nonradiative process is ISC. The T_1 states of **3a**, **3c** and **4** are of π,π^* with CT character while that of **3b** is of n,π^* . Therefore, the variation in the ISC rates of **3a-c** and **4** is reasonably explained by El-Sayed's selection rule. The spectroscopic properties of **2-4** were also correlated to the DFT calculation data. The obtained results and mechanistic explanations on the processes from the S_1 states of **2-4** will be useful on designing new fluorescent TPy derivatives for applications as fluorophores.

Acknowledgements

This work was supported by a Grant-in-Aid for Scientific Research C (No. 22550031) from the Japan Society for the Promotion of Science. Financial support was also provided by the Iketani Science and Technology Foundation and Izumi Science and Technology Foundation. We thank the Information Technology Center of the University of Electro-Communications for technical assistance in computing the quantum chemical calculations.

Supplementary data

Transient absorption and DFT calculation data associated with this article can be found as Electronic Supplementary Information (ESI), in the online version, at doi:###.

References

1. O. Shimomura, *Bioluminescence: Chemical Principles and Methods*, rev. ed., World Scientific, Singapore, 2012.
2. (a) T. Goto, Chemistry of bioluminescence, *Pure Appl. Chem.*, 1968, **17**, 421–441; (b) T. Goto and H. Fukatsu, Cypridina bioluminescence 7. Chemiluminescence in micelle solutions— A model system for Cypridina bioluminescence, *Tetrahedron Lett.*, 1969, 4299–4302.
3. T. Hirano, T. Nakagawa, A. Kodaka, S. Maki, H. Niwa and M. Yamaji, 5-[4-(Dimethylamino)phenyl]-2-benzamidopyrazines: fluorescent dyes based on Cypridina oxyluciferin, *Res. Chem. Intermed.*, 2013, **39**, 233–245.
4. Textbooks: (a) R. Y. Tsien, *Fluorescent Chemosensors for Ion and Molecule Recognition*, ed. A. W. Czarnik, ACS: Washington, DC, 1993, pp. 130–146; (b) H. Zollinger, *Color Chemistry: Syntheses, Properties, and Applications of Organic Dyes and Pigments*, 3rd ed., Wiley-VCH: Weinheim, 2003; (c) *Industrial Dyes: Chemistry, Properties, Applications*, ed. K. Hunger,, Wiley-VCH: Weinheim, 2003; (d) B. Valeur and M. N. Berberan-Santos, *Molecular Fluorescence: Principles and Applications*, 2nd ed., Wiley-VCH: Weinheim, 2013.
5. T. Hirano, Y. Takahashi, H. Kondo, S. Maki, S. Kojima, H. Ikeda and H. Niwa, The reaction mechanism for the high quantum yield of the *Cypridina* (*Vargula*) bioluminescence supported by chemiluminescence of 6-aryl-2-methylimidazo[1,2-*a*]pyrazin-3(7*H*)-ones (Cypridina luciferin analogues), *Photochem. Photobiol. Sci.*, 2008, **7**, 197–207.
6. S. Hachiya, T. Inagaki, D. Hashizume, S. Maki, H. Niwa, T. Hirano, Synthesis and fluorescence properties of difluoro[amidopyrazinato-*O,N*]boron derivatives: a new boron-containing fluorophore, *Tetrahedron Lett.*, 2010, **51**, 1613–1615.
7. C. Fruit, A. Turck, N. Ple, G. Queguiner, Syntheses of *N*-diazinyl thiocarboxamides and of thiazolodiazines. Metalation studies. Diazines XXXIII, *Hetrocyclic Chem.* 2002, **39**, 1077–1082.

8. (a) G. B. Barlin, Purine analogs as amplifiers of phleomycin. VIII Some thiazolo[4,5-*b*]pyrazines and related-compounds, *Aust. J. Chem.*, 1983, **36**, 983–992; (b) G. B. Barlin, S. J. Ireland, B. J. Rowland, Purine analogues as amplifiers of phleomycin. IX Some 2- and 6-substituted thiazolo[4,5-*b*]pyrazines, 2-substituted thiazolo[4,5-*c*]- and thiazolo[5,4-*b*]pyridines and related compounds, *Aust. J. Chem.*, 1984, **37**, 1729–1737; (c) B. Koren, B. Stanovik, M. Tisler, Transformations of 1,2,4-thiadiazolo/2,3-*x*/azines, *Heterocycles*, 1987, **26**, 689–697.
9. (a) R. C. Phadke and D. W. Rangnekar, Synthesis of 2-(alkyl and aryl)thiazolo[4,5-*b*]quinoxaline derivatives and study of their fluorescent properties, *Bull. Chem Soc. Jpn.*, 1986, **59**, 1245–1247; (b) A. R. Katritzky and W. Q. Fan, Some novel quinone-type dyes containing naphthoquinone and related fused ring systems, *J. Heterocycl. Chem.*, 1988, **25**, 901–906; (c) R. C. Phadke, D. W. Rangnekar, Synthesis of 1,4-Dioxino[2,3-*b*]quinoxaline derivatives and a study of their fluorescent properties, *Dyes Pigment.*, 1989, **10**, 159–164; (d) M. Matsuoka, A. Iwamoto, N. Furukawa and T. Kitao, Syntheses of polycyclic-1,4-dithiins and related heterocycles, *J. Heterocycl. Chem.*, 1992, **29**, 439–443; (e) D. W. Rangnekar, N. D. Sonawane and R. W. Sabnis, Synthesis of 2-styrylthiazolo[4,5-*b*]quinoxaline based fluorescent dyes, *J. Heterocycl. Chem.*, 1998, **35**, 1353–1356; (f) S. A. Khan, Synthesis, characterization and *in vitro* antibacterial activity of new steroidal 5-en-3-oxazolo and thiazoloquinoxaline, *Eur J. Med. Chem.* 2008, **43**, 2040–2044; (g) M. Shaikh, J. Mohanty, P. K. Singh, A. C. Bhasikuttan, R. N. Rajule, V. S. Satam, S. R. Bendre, V. R. Kanetkar and H. Pal, Contrasting solvent polarity effect on the photophysical properties of two newly synthesized aminostyryl dyes in the lower and in the higher solvent polarity regions, *J. Phys. Chem. A*, 2010, **114**, 4507–4519; (h) Y. A. Sonawane, R. N. Rajule, and G. S. Shankarling, Synthesis of novel diphenylamine-based fluorescent styryl colorants and study of their thermal, photophysical, and electrochemical properties, *Monatsh. Chem.*, 2010, **141**, 1145–1151.
10. M. Yamaji, Y. Aihara, T. Itoh, S. Tobita and H. Shizuka, Thermochemical profiles on hydrogen atom transfer from triplet naphthol and proton-induced electron transfer from triplet methoxynaphthalene to benzophenone via triplet exciplexes studied by laser flash

- photolysis, *J. Phys. Chem.*, 1994, **98**, 7014–7021.
11. M. J. Frisch, G. W. Trucks, H. B. Schlegel, G. E. Scuseria, M. A. Robb, J. R. Cheeseman, G. Scalmani, V. Barone, B. Mennucci, G. A. Petersson, H. Nakatsuji, M. Caricato, X. Li, H. P. Hratchian, A. F. Izmaylov, J. Bloino, G. Zheng, J. L. Sonnenberg, M. Hada, M. Ehara, K. Toyota, R. Fukuda, J. Hasegawa, M. Ishida, T. Nakajima, Y. Honda, O. Kitao, H. Nakai, T. Vreven, J. A. Montgomery, Jr., J. E. Peralta, F. Ogliaro, M. Bearpark, J. J. Heyd, E. Brothers, K. N. Kudin, V. N. Staroverov, R. Kobayashi, J. Normand, K. Raghavachari, A. Rendell, J. C. Burant, S. S. Iyengar, J. Tomasi, M. Cossi, N. Rega, J. M. Millam, M. Klene, J. E. Knox, J. B. Cross, V. Bakken, C. Adamo, J. Jaramillo, R. Gomperts, R. E. Stratmann, O. Yazyev, A. J. Austin, R. Cammi, C. Pomelli, J. W. Ochterski, R. L. Martin, K. Morokuma, V. G. Zakrzewski, G. A. Voth, P. Salvador, J. J. Dannenberg, S. Dapprich, A. D. Daniels, Ö. Farkas, J. B. Foresman, J. V. Ortiz, J. Cioslowski and D. J. Fox, Gaussian, Inc., Wallingford CT, 2009.
12. (a) A. D. Becke, Density-functional thermochemistry 3. The role of exact exchange, *J. Chem. Phys.*, 1993, **98**, 5648–5652; (b) C. T. Lee, W. T. Yang and R. G. Parr, Development of the Colle-Salvetti correlation-energy formula into a functional of the electron-density, *Phys. Rev. B*, 1988, **37**, 785–789; (c) P. J. Stephens, F. J. Devlin, C. F. Chabalowski and M. J. Frisch, Ab-initio calculation of vibrational absorption and circular-dichroism spectra using density-functional force-fields, *J. Phys. Chem.*, 1994, **98**, 11623–11627.
13. R. Dennington, T. Keith and J. Millam, Semichem Inc., Shawnee Mission KS, Version 5, 2009.
14. C. Reichardt, *Solvents and Solvent Effects in Organic Chemistry*, 3rdn, Wiley-VCH, Weinheim, 2003.
15. S. J. Strickler and R. A. Berg, Relationship between absorption intensity and fluorescence lifetime of molecules, *J. Phys. Chem.*, 1962, **37**, 814–822.
16. (a) M. A. El-Sayed, Radiationless processes involving change of multiplicity in the diazenes, *J. Chem. Phys.*, 1962, **36**, 573–574; (b) M. A. El-Sayed, Spin-orbit coupling and the radiationless processes in nitrogen heterocyclics, *J. Chem. Phys.*, 1963, **38**,

2834–2838.

Graphical Abstract

Substituent effects on fluorescence properties of thiazolo[4,5-*b*]pyrazine derivatives

Tatsuki Nakagawa, Minoru Yamaji, Shojiro Maki, Haruki Niwa and Takashi Hirano*

Fluorescence properties of thiazolo[4,5-*b*]pyrazine derivatives having the phenyl group at C2 prepared from amidopyrazines were studied, to show that introduction of electron-donating groups onto the 2-phenyl moiety is operative for increasing the fluorescence yield and appearance of solvatochromic character.

